Int. J. Multiphase Flow Vol. 11, No. 2, pp. 213–239, 1985
Printed in the U.S.A.

0301-9322/85 $3.00 + .00

TRANSPORT PROCESSES IN FRACTALS

II. STOKES FLOW IN FRACTAL CAPILLARY NETWORKS

P. M. ADLER
Laboratoire d'Aérothermique, 4 ter, Route des Gardes, 92190-Meudon, France

(*Received* 20 *December* 1983; *in revised form* 23 *July* 1984)

Abstract—General fractal capillary networks are constructed and described via a systematic use of algebraic graph theory. The Stokes flow problem is then addressed in this contribution; the matrix relating the flow rates to the pressures is obtained through a general iteration formula, which is deduced from the algebraic description of the geometrical structure. This formula is generally nonlinear; it is only in the limit of a large number of iterations that it can be linearized and that a fractal exponent can be obtained. Two examples are provided to illustrate the formal developments. Various aspects of the results are then discussed and the permeability of a spatially periodic network whose unit cell is a fractal calculated.

1. INTRODUCTION

In the first part of this series (Adler 1984), the transport properties of a Leibniz packing were calculated in the lubrication limit. In consequence of its structural simplicity, the packing was compared to an electrical network and the equivalent resistances and conductances could be derived by elementary means such as the star-triangle transformation.

In this issue, we wish to describe a general class of fractal structures, which consist of capillary networks and to calculate the flow and the pressure inside such a network. The practical, and potential, background of such a contribution is obviously related first to natural porous media, which are often schematized by consolidated arrays of interconnected capillary tubes. Moreover, most porous media can be considered as homogeneous at a macroscopic length scale, but heterogeneous at a local scale. The global homogeneity is related to the global translational invariance at this scale, while the local heterogeneity is itself related to a local dilational invariance. This dilational invariance can be schematized by a fractal structure. For instance, a percolating network is fractal at small scale (see Stauffer 1979). Potential applications to the analysis of two-phase flows through porous media may also be foreseen at least in connection with the percolation aspect of this situation (Larsen *et al.* 1981, De Gennes & Guyon 1978).

Thus, a natural link exists between this issue and a previous series devoted to spatially periodic capillary networks (Adler & Brenner 1984 a, b and c). They nicely complement each other in view of the potential applications to porous media, which are mentioned above. The basic graph of the spatially periodic capillary network would then consist of a fractal structure. Hence, the reader will be provided with a fairly complete analysis of both structures and with a general formalism.

Another attractive feature of networks is a consequence of the fact that they are relatively easy to analyze when compared to continuum situations where partial differential equations have to be solved. But the basic quantities of interest do have the same behaviour, whether they are continuous or discrete. For instance, the flow rates (or the velocity field) in a spatially periodic medium are spatially periodic as a result of the geometric periodicity of the medium. The analogous feature is expected to occur here, since it is geometric in nature. Thus, the solution of a discrete situation will hopefully suggest and support the basic assumptions which can be made for continuous fields.

To the best of our knowledge, there have been no similarly oriented contributions. Certainly, Mandelbrot's book (1982) constitutes the most fascinating introduction to the field. In addition to the references cited in the first part of this series (Adler 1984), the following ones devoted to superconductivity of networks may be of interest here, Alexander (1983) and Rammal *et al.* (1983 a and b).

This paper is organized as follows. The second section is devoted to the description and definition of a fractal capillary network, which is assumed to be self-similar. The general definition due to Hutchinson (1981) is transposed to the present case; mathematically speaking, an invariant compact set can be viewed as a union of images of itself by contraction maps. In continua, the geometry generally imposes severe constraints, which can be skipped in discrete situations. A discrete fractal may be constructed with two ingredients; we start with a given finite graph Γ_0, called the basic graph. Then, a new graph Γ_1 is obtained by combining a finite number of basic graphs Γ_0 according to a given recipe. A second graph Γ_2 can be generated when the graphs Γ_1 are combined according to the same recipe as before. This process can be indefinitely continued and a self-similar fractal is generated. An algebraic analysis of the construction process is offered.

In section 3, the Stokes flow of a Newtonian fluid in the capillary network symbolised by the basic graph Γ_0 is analyzed. This provides us with the opportunity to recall some elementary properties of this linear problem and to make clear the analogy between it and its electrical counterpart. A transfer matrix $\mathbf{A}_0$ is introduced; it relates the flow rates and the pressures at the external vertices of the basic graph Γ_0

The central section of this paper is 4, where the Stokes problem is solved on the fractal graph Γ_N; it depends upon both the initial graph Γ_0 and the construction process. The transfer matrix $\mathbf{A}_N$ which relates the flow rates and the pressures at the external vertices of the graph Γ_N are explicitly calculated by means of linear algebra, making a full use of the algebraic description of Γ_N. The major result of this section is the derivation of a general iteration formula between $\mathbf{A}_N$ and $\mathbf{A}_{N-1}$, which turns out to be nonlinear. It is only in the limit, i.e. near fixed points when they exist, that this expression can be linearized; it yields the so-called linear fractal relation between two successive generations. Hence a clear distinction is drawn between the general nonlinear regime and the final fractal regime.

In order to illustrate the previous abstract developments, section 5 is devoted to the detailed treatment of two examples. The first one is the classical Sierpinski gasket; an application of the general formula yields the usual 3/5 constant; in this case, the linear character of the relation is a consequence of the isotropy, since an anisotropic gasket yields a nonlinear relation. The second example tentatively describes the injection of a fluid inside a porous medium; it is also reminiscent of the structure of polymers adsorbed on a solid surface.

All the results are briefly discussed in section 6. The construction of the network can be generalized in several ways, as it was noticed in connection with the second example. The formal structure of the result is compared to the one obtained in a spatially periodic network. The fractal properties of the various quantities of interest are analyzed in view of their applications to continuous fields. The interaction between anisotropy and nonlinearity is briefly discussed. Finally, the permeability of a spatially periodic network, whose basic graph is a fractal is calculated.

In view of the abstract character of the following developments, the reader may find it useful to have general references on the subject and an alternative way to read this paper. A general introduction to algebraic graph theory has been written by Biggs; however, some of it is presented in a previous paper of Adler & Brenner (1984 a) for spatially periodic networks. The reader may skip the first few sections and go directly to section 5 which is devoted to two examples of fractals; his geometrical insight may of course be stimulated by Mandelbrot (1982). Then, he can come back to the first sections of this paper.

2. GEOMETRICAL DESCRIPTION OF A FRACTAL CAPILLARY NETWORK

Hutchinson (1981) defined an invariant compact set $K \subseteq \mathbb{R}^n$ as a set such that

$$K = \bigcup_{\alpha=1}^{M} S_\alpha K, \qquad [1]$$

where $\{S_\alpha, \alpha = 1 \ldots M\}$ is a finite family of contraction maps on $\mathbb{R}^n$. Often, but not always the S_α are similitudes.

Hutchinson (1981) also gave some examples such as the Cantor set and the Koch curve which clearly show how the final invariant set K may be constructed by successive applications of the family contractions.

The fractal capillary network is constructed in a similar manner here. We shall start with an elementary graph Γ_0 which is called the basic graph. Then a finite family of transformations S_α is applied to Γ_0; M finite graphs $S_\alpha\Gamma_0$ are obtained, which are connected in a specified way. A new graph Γ_1 is obtained and the previous process may be applied again. This is illustrated in figure 1.

Let us first describe the basic graph Γ_0. The minimum amount of graph terminology is introduced when needed; most of it was already used by Adler & Brenner (1984 a, b, and c). Note that an excellent introduction to algebraic graph theory has been written by Biggs (1974).

A finite capillary network may be schematized by a finite graph Γ_0, when a clearcut distinction exists between the junctions themselves and the capillaries connecting them. In place of the physical terms "junctions" and "capillaries," we shall employ the graph terms "vertices" and "edges," respectively. Hence, Γ_0 may be considered as

$$\begin{aligned} &\text{a set } V\Gamma_0 \text{ of } n \text{ vertices } v_i \text{ connected by} \\ &\text{a set } E\Gamma_0 \text{ of } m \text{ edges } e_j \end{aligned} \qquad [2]$$

The relations between vertices may be represented by the adjacency matrix $\mathcal{A}$ of the graph, and the relations between vertices and edges by the incidence matrix **D** (cf. Biggs 1974 for a complete definition).

Γ_0 is assumed to be connected, i.e. every pair of vertices may be joined by a walk.

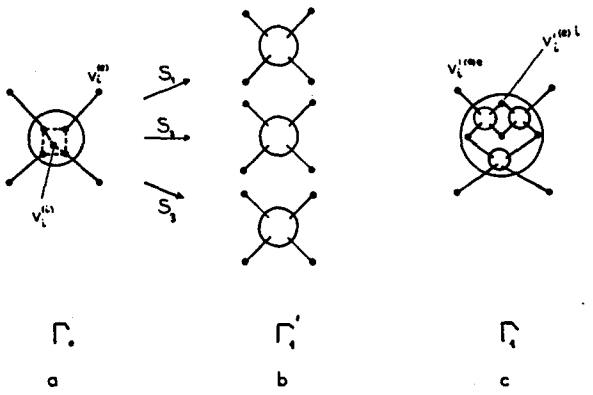

Figure 1. Construction of a fractal. (a) The basic graph Γ_0 with its n_e external vertices $v_i^{(e)}$ and its $n - n_e$ internal vertices $v_i^{(i)}$. (b) The transformations $S_\alpha(\alpha = 1, \ldots, M)$ yield the graph Γ_1' made of the juxtaposition of the M transformed graphs $S_\alpha\Gamma_0$. (c) These graphs are then interconnected in a specified way to form the graph Γ_1. Note the distinction between the external vertices $v_i'^{(e)i}$ of Γ_1' which become internal vertices of Γ_1, and the external vertices $v_i'^{(e)e}$ of Γ_1' which become external vertices of Γ_1.

Two kinds of vertices are distinguished in Γ_0 (cf. figure 1a):

$$\begin{aligned} &n_e \text{ external vertices } v_i^{(e)}, \\ &n - n_e \text{ internal vertices } v_i^{(i)}. \end{aligned} \qquad [3]$$

Of course, the external vertices are connected to external pressure generators and are the vertices by which flow rates go in and out the piece of porous material symbolised by Γ_0. We shall come back to this point in section 3.

Algebraically, a projection operator $\mathbf{H}^{o,e}$ can be defined on $V\Gamma_0$ as a square $n \times n$ matrix where only the diagonal elements may be nonzero:

$$H_{ii}^{o,e} = \begin{cases} 1 & \text{if } v_i \text{ is an external vertex,} \\ 0 & \text{otherwise.} \end{cases} \qquad [4]$$

Hence, on $V\Gamma_0$, the vector $\mathbf{v}^{(e)}$ corresponding to the external vertices may be obtained as

$$\mathbf{v}^{(e)} = \mathbf{H}^{o,e} \cdot \mathbf{1}, \qquad [5]$$

where $\mathbf{1}$ denotes the vector $\overbrace{(1 \cdots 1)}^{n}\dagger$ on $V\Gamma_0$.

Consider a given family of transformations S_α ($\alpha = 1, \ldots M$) which act on the basic graph Γ_0, in a manner which will be specified later. The construction of the graph Γ_1 requires two steps (cf. figure 1). First the graph Γ_1' is defined as the juxtaposition of the graphs $S_\alpha \Gamma_0$

$$\Gamma_1' = \bigcup_{i=1}^{M}{}' S_\alpha \Gamma_0, \qquad [6]$$

where $\bigcup'$ denotes the juxtaposition without any interconnections between the external vertices of the graphs $S_\alpha \Gamma_0$.

Second the external vertices of the elementary graphs $S_\alpha \Gamma_0$ are connected one to the other one in a specified way

$$\Gamma_1 = \bigcup_{i=1}^{M} S_\alpha \Gamma_0, \qquad [7]$$

where $\bigcup$ stands for the interconnections.

Let us assume that the interconnections are defined in such a way as to leave n_e external vertices to the graph Γ_1. Hence, the process can be indefinitely continued; Γ_N may be expressed as

$$\Gamma_N = \bigcup_{\alpha=1}^{M} S_\alpha \Gamma_{N-1}. \qquad [8]$$

Note here that the cartesian concept of coordinates can be generalized to fractals in the following way. In Γ_1, a given graph $S_\alpha \Gamma_0$ can be determined without any ambiguity by the integer α of S_α. After N generations, $S_{\alpha_N} \cdots S_{\alpha_i} \cdots S_{\alpha_1} \Gamma_0$, may be simply referred to by the sequence of the N integers ranging from 1 to M

$$\{\alpha_1 \cdots \alpha_i \cdots \alpha_N\}. \qquad [9]$$

Further technical details may be found in Hutchinson (1981).

This localisation of a part of a fractal by a sequence of integers may be usefully compared to the localisation of a part of a spatially periodic medium by three integers in $\mathbb{R}^3$ (cf. Adler & Brenner 1984 a).

We shall not insist very much on the transformations S_α, which can belong to a very large class. Usually, S_α consists of the multiplication of all the lengths involved in a given geometry by a factor λ. For instance, in the usual three dimensional space $\mathbb{R}^3$, the length of a capillary is multiplied by λ and its section by λ^2. However, more complex rules of the game may be given and one is only limited by the physical relevance of the chosen transformation; edges may be delected or added and so on. A large class of transformations S_α may be represented by a linear relation between the transfer matrix of Γ_0 and the transfer matrix of $S_\alpha \Gamma_0$, as it is detailed in section 4.

In the rest of this section, we shall be exclusively concerned with the connections between the external vertices of the various $S_\alpha \Gamma_0$ and by their algebraic representation.

In order to remain as simple as possible, the following restrictions are made on these connections.

It is assumed that an external vertex of $S_\alpha \Gamma_0$ may either become an external vertex of Γ_1 or be connected to another external vertex of $S_{\alpha'} \Gamma_0$. Hence, connections between external and internal vertices of different subgraphs are forbidden. Moreover, an external vertex of $S_\alpha \Gamma_0$ cannot be left dangling. Multiple connections between three or more external vertices are not allowed.

Certainly, these restrictions could be removed without any serious troubles and could be taken into account by simple modifications of the algebraic manipulations. However, this would bring into the theory unnecessary complications which would obscure its meaning.

The connection between various external vertices of the graphs $S_\alpha \Gamma_0$ is equivalent to the superposition of some of the Mn_e external vertices of the graph Γ_1'. Since Γ_1 is required to possess n_e external vertices, it turns out on elementary grounds that $(M-1)n_e$ must be an even number.

Let us now algebraically describe the superposition of some of the Mn_e external vertices of the graph Γ_1'. First a clear distinction must be drawn between the $Mn_e - n_e$ external vertices of Γ_1' which become internal vertices of Γ_1 (they are denoted by $v_i'^{(e)i}$) and the n_e external vertices of Γ_1' which become the n_e external vertices of Γ_1 (they are denoted by $v_i'^{(e)e}$). This is illustrated in figure 1c.

Two projection operators can be defined when necessary on the vertex space $V\Gamma_1'$. $\mathcal{P}'^{(i)}$ is the projection on the vertices of Γ_1' which becomes internal; $\mathcal{P}'^{(e)}$ is the projection on the vertices of Γ_1' which become the external vertices of Γ_1. The definition of the corresponding $Mn_e \times Mn_e$ matrices $\mathcal{P}'^{(i)}$ and $\mathcal{P}'^{(e)}$ parallels the relation [4].

On the vertex space $V\Gamma_1'^{(e)i}$ of the $(M-1)n_e$ vertices $v_i'^{(e)i}$, the superposition of two vertices may be symbolized by the $(M-1)n_e \times (M-1)n_e$ matrix $\mathcal{T}$ defined as

$$\begin{aligned} &\mathcal{T}_{ij} = 1 \text{ when the vertices } v_i'^{(e)i} \text{ and } v_j'^{(e)i} \text{ are superposed,} \\ &\mathcal{T}_{ij} = 0 \text{ otherwise.} \end{aligned} \qquad [10]$$

Note that $\mathcal{T}$ completely describes the transformation of Γ_1' into Γ_1. $\mathcal{T}$ has many elementary properties as a consequence of its definition and of the restrictions placed upon the transformation of Γ_1' into Γ_1. It is symmetric. It has only one 1 in each line and each column. The repeated application of two transformations $\mathcal{T}$ on the vertex space $V\Gamma_1'^{(e)}$ yields the initial vertices; hence $\mathcal{T}$ is idempotent and is its own inverse

$$\mathcal{T}^2 = \mathbf{I}, \quad \mathcal{T} = \mathcal{T}^{-1}. \qquad [11]$$

$\mathcal{T}$ has no diagonal element, which would correspond to a forbidden dangling vertex.

This matrix is illustrated at length in section 5, to which the reader is referred.

An important condition is imposed on Γ_1; it is assumed to be connected, i.e. every pair of vertices of Γ_1 may be joined by a walk. The condition for this property to hold may be expressed as follows. Instead of using the detailed relation [10], a new graph Γ_1'' may be defined. Γ_1'' contains M vertices $\{v_\alpha''; \alpha = 1, \ldots, M\}$, which correspond to the M subgraphs $\{S_\alpha \Gamma_0; \alpha = 1, \ldots, M\}$ of Γ_1. Two vertices v_α'' and v_β'' of Γ_1'' are connected by an edge if the subgraphs $S_\alpha \Gamma_0$ and $S_\beta \Gamma_0$ have a common external vertex. The adjacency matrix $\mathcal{A}_1''$ (cf. Biggs 1974, p. 9) of this new graph Γ_1'' may be introduced. Since Γ_0 is connected, the connectivity of Γ_1 is obviously equivalent to the connectivity of Γ_1''. It is known as a general result from graph theory (cf. Biggs 1974, p. 13) that Γ_1'' is connected if and only if $(\mathcal{A}_1'' + \mathbf{I})^M$ has no zero entries.

This terminates the general description of a fractal capillary network. It is useful to note that our fractal definition does not allow relations between subgraphs which are not nearest neighbours, so to speak. Relations are only permitted between graphs of the same generation.

It is always fruitful to make a parallel between the fractal and the spatially periodic characters. The basic graph Γ_0 plays the same role in both situations, hence its name. The matrix $\mathcal{T}$ stands for the relations between the unit cell and its neighbours in the spatially periodic case. Hence, the restriction just mentioned about fractal networks is equivalent to a spatially periodic graph where only nearest—neighboured cells are interrelated.

3. STOKES FLOW ON THE BASIC GRAPH

This section is devoted to the elementary analysis of Stokes flow on the basic graph Γ_0. Of course, it is well known and described in many references (see for instance Biggs 1974 and Bollobàs 1979). The basic features of these solutions are given.

Consider the piece of porous medium symbolized by the graph Γ_0. *A priori*, we are only interested by the relation between the flow rates going in and out of the material, and the pressures imposed at the external vertices (figure 2a). This relation is linear when the fluid is Newtonian and when the Reynolds number is everywhere vanishingly small.

To each external vertex of Γ_0 can be associated a pressure and a flow rate, with the arbitrary convention that the flow rate is positive when it goes out of Γ_0. Hence, the n_e pressures and the n_e flow rates can be represented by the vectors $\mathbf{P}_0^{(e)}$ and $\mathbf{J}_0^{(e)}$, respectively, which are defined on the space of the external vertices $V\Gamma_0^{(e)}$. The linear relation between these two vectors may be expressed as

$$\mathbf{J}_0^{(e)} = \frac{1}{\mu} \mathbf{A}_0 \cdot \mathbf{P}_0^{(e)}, \qquad [12]$$

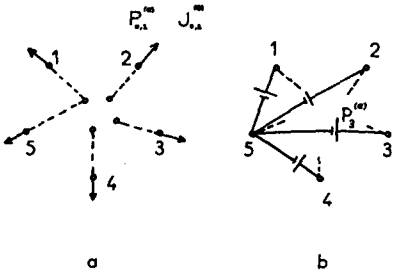

Figure 2. Stokes flow on the basic graph Γ_0. (a) The external vertices 1 to 5 are represented together with the corresponding pressures $P_{0i}^{(e)}$ and outgoing flow rates $J_{0i}^{(e)}$ ($i = 1, \ldots, 5$). (b) The graph γ_0 on which the matrix $\mathbf{a}_0$ [cf. [15]] is determined by use of standard methods of graph theory. Generators whose strength is equal to the relative pressures are positioned between $n_e - 1$ external vertices and for instance the last one.

where $\mathbf{A}_0$ is a $n_e \times n_e$ matrix, that we call the transfer matrix of the graph Γ_0. μ is the viscosity of the fluid.

$\mathbf{A}_0$ is generally symmetric, as it will be shown later, but it is noninvertible for the following reasons (its rank is actually equal to $n_e - 1$). First, the flow rates do not vary when an arbitrary constant is added to the pressures; hence,

$$\mathbf{A}_0 \cdot \mathbf{1} = 0, \qquad [13a]$$

where $\mathbf{1}$ denotes the vector $\overbrace{(1 \ldots 1)}^{n_e}\dagger$ on $V\Gamma_0^{(e)}$. Second, the sum of the outgoing flow rates is equal to zero, as a direct consequence of the conservation of the flow rates at each vertex of the graph Γ_0. Hence,

$$\mathbf{1}\dagger \cdot \mathbf{A}_0 = 0 \qquad [13b]$$

which is identical to [13a] since $\mathbf{A}_0$ is symmetric.

This unessential undeterminacy can be removed by choosing an arbitrary vertex, say the last one $v_{n_e}^{(e)}$, which is assumed to be at a zero pressure. Moreover, the flux $J_{0,n_e}^{(e)}$ is given by

$$J_{0,n_e}^{(e)} = -\sum_{i=1}^{n_e-1} J_{0,i}^{(e)}. \qquad [14]$$

The remaining unknowns $(J_{0,i}^{(e)};\ i = 1, \ldots, n_e - 1)$ and $(P_{0,i}^{(e)};\ i = 1, \ldots, n_e - 1)$ may be represented by the vectors $\mathbf{j}_0^{(e)}$ and $\mathbf{p}_0^{(e)}$, respectively. They are linked by the linear relation

$$\mathbf{j}_0^{(e)} = \frac{1}{\mu}\mathbf{a}_0 \cdot \mathbf{p}_0^{(e)}, \qquad [15]$$

where $\mathbf{a}_0$ is an $(n_e - 1) \times (n_e - 1)$ invertible and symmetric matrix.

$\mathbf{a}_0$ can be calculated by a direct application of a process described for instance by Bollobas (1979). Equation [15] actually corresponds to the situation illustrated in figure 2b. Additional edges are added between the first $n_e - 1$ external vertices and the last one n_e; pressure generators, whose strength is equal to the relative pressures, are supposed to be located along these edges.

Three sets of equations are written on this new graph γ_0, which has n vertices and $m + n_e - 1$ edges. The conservation of the total flow rate is expressed at each vertex. The pressure difference is zero along every cycle of the graph γ_0. Finally, the pressure difference between two adjacent vertices i and i' is proportional to the flow rate $J(j)$ between these vertices. Explicitly,

$$p(i) - p(i') = \mu\, s(j)\, J(j), \qquad [16]$$

where j is the number of the oriented edge $\{i, i'\}$. $s(j)$ is the "pressure drop-flow rate conductivity" coefficient along the edge j. When the capillary j is a cylinder of radius $R(j)$ and length $L(j)$, the Poiseuille's law applies (Happel & Brenner 1965) and $s(j)$ can be expressed as

$$s(j) = \frac{8}{\pi} \cdot \frac{L(j)}{R^4(j)}. \qquad [17]$$

It is interesting to note that, when all the dimensions are multiplied by a factor λ, $s(j)$ is multiplied by λ^{-3}.

The three mentioned sets of equations enable us to express the flow rate vector $\mathbf{j}_0$ (defined on the edge space of γ_0) as (Biggs 1974)

$$\mathbf{j}_0 = -\frac{1}{\mu}\mathbf{C}\cdot(\mathbf{C}\dagger\cdot\mathbf{M}\cdot\mathbf{C})^{-1}\cdot\mathbf{C}\dagger\cdot\mathbf{z}, \qquad [18]$$

where $\mathbf{M}$ is a $(m + n_e - 1) \times (m + n_e - 1)$ conductance matrix whose the first m diagonal elements are equal to the resistances $s(j)$. $\mathbf{C}$ is the $(m + n_e - 1) \times (m + n_e - n)$ cycle matrix of γ_0 (cf. Biggs 1974, p. 31). $\mathbf{Z}$ is the voltage vector; here, its components are zero except on the last $n_e - 1$ additional edges where they are equal to $\mathbf{p}_{0,i}^{(e)}$.

Hence, $\mathbf{a}_0$ is readily deduced as a submatrix of [18] from which its symmetric character follows. Note that it is also negative definite.

It is easy to show that $\mathbf{A}_0$ may be derived from $\mathbf{a}_0$ as

$$\mathbf{A}_0 = \begin{array}{c} \\ n_e - 1 \\ 1 \end{array}\begin{array}{c} \overset{n_e-1}{\longleftrightarrow} \quad \overset{1}{\longleftrightarrow} \\ \begin{pmatrix} \mathbf{a}_0 & -\mathbf{a}_0\cdot\mathbf{1} \\ -\mathbf{1}\dagger\cdot\mathbf{a}_0 & \mathbf{1}\dagger\cdot\mathbf{a}_0\cdot\mathbf{1} \end{pmatrix} \end{array}, \qquad [19]$$

where $\mathbf{1}$ denotes the vector $\overbrace{(1\ldots1)}^{n_e-1}\dagger$. The requirements [13] are obviously satisfied by $\mathbf{A}_0$.

As a conclusion of this section, both formulations [12] and [15] are of course correct. As it is shown by [18], [15] is usually the most natural starting point, especially when Γ_0 is a complicated graph. In the following, [12] is usually used though it is not invertible. A last important feature of $\mathbf{A}_0$ and $\mathbf{a}_0$ is that they only depend upon the geometry of the network.

4. STOKES FLOW ON THE FRACTAL CAPILLARY NETWORK

4.1. *Basic relations*

Let us denote by $\mathbf{J}_1^{(e)}$ the vector defined on the subspace $V\Gamma_1^{(e)}$ of the external vertices of Γ_1; $\mathbf{J}_1^{(e)}$ represents the n_e flow rates going out of Γ_1. Similarly, the n_e pressures at these vertices are represented by the vector $\mathbf{P}_1^{(e)}$. Paralleling [12] and [15], the following relations hold for these two vectors

$$\mathbf{J}_1^{(e)} = \frac{1}{\mu}\mathbf{A}_1\cdot\mathbf{P}_1^{(e)} \qquad [20a]$$

or equivalently,

$$\mathbf{j}_1^{(e)} = \frac{1}{\mu}\mathbf{a}_1\cdot\mathbf{p}_1^{(e)}. \qquad [20b]$$

One of the major purposes of the present paper is to calculate in a general and convenient form these matrices $\mathbf{A}_1$ and $\mathbf{a}_1$ as a function of the structure of the basic graph Γ_0 represented by its matrices $\mathbf{A}_0$ or $\mathbf{a}_0$, as a function of the family of transformation $S_\alpha(\alpha = 1, \ldots, M)$ and as a function of the interconnection between the graphs $S_\alpha\Gamma_0$ $(\alpha = 1, \ldots, M)$ represented by the matrix $\mathcal{T}$. This relation may be expressed as

$$\mathbf{A}_1 = \mathbf{F}_{s,\mathcal{T}}(\mathbf{A}_0), \qquad [21a]$$

$$\mathbf{a}_1 = \mathbf{F}_{s,\mathcal{T}}(\mathbf{a}_0), \qquad [21b]$$

where $\mathbf{F}_{s,\mathcal{T}}$ and $\mathbf{f}_{s,\mathcal{T}}$ are two tensorial functions which will be determined.

More generally, this calculation can be extended to any iteration of rank N

$$\mathbf{J}_N^{(e)} = \frac{1}{\mu} \mathbf{A}_N \cdot \mathbf{P}_N^{(e)} \qquad [22a]$$

or equivalently,

$$\mathbf{j}_N^{(e)} = \frac{1}{\mu} \mathbf{a}_N \cdot \mathbf{p}_N^{(e)}, \qquad [22b]$$

where, by a straightforward application of [21],

$$\mathbf{A}_N = \mathbf{F}(\underbrace{\cdots \mathbf{F}(\mathbf{A}_0) \cdots}_{N}). \qquad [23]$$

Advantage will also be taken of this general structure to give some of the major field properties which can be expected in the continuous case and which will be used in a future outcome of the present series.

4.2. *Description of the assemblages*

Let us recall first that Γ_1' was defined by [6] as the juxtaposition without interconnections of the M subgraphs $S_\alpha \Gamma_0$. An external flow rate vector $\mathbf{J}_1'^{(e)}$ can be defined on the space $V\Gamma_1'^{(e)}$ of all the external vertices of the graph Γ_1'; of course, $V\Gamma_1'^{(e)}$ is simply the union of all the external vertices of the transformed subgraphs $S_\alpha \Gamma_0$ ($\alpha = 1, \ldots, M$); hence,

$$V\Gamma_1'^{(e)} = \bigcup_{\alpha=1}^{M} S_\alpha (V\Gamma_0^{(e)}). \qquad [24]$$

$\mathbf{J}_1'^{(e)}$ is thus given by

$$\mathbf{J}_1'^{(e)} = \begin{pmatrix} S_1 & \mathbf{J}_0^{(e)} \\ \vdots & \\ S_\alpha & \mathbf{J}_0^{(e)} \\ \vdots & \\ S_M & \mathbf{J}_0^{(e)} \end{pmatrix} \qquad [25a]$$

and similarly,

$$\mathbf{P}_1'^{(e)} = \begin{pmatrix} S_1 & \mathbf{P}_0^{(e)} \\ \vdots & \\ S_\alpha & \mathbf{P}_0^{(e)} \\ \vdots & \\ S_M & \mathbf{P}_0^{(e)} \end{pmatrix} \qquad [25b]$$

On the graph Γ_1', which is generally disconnected, the relation between the flow rate vector $\mathbf{J}^{\prime(e)}$ and the external pressure vector $\mathbf{P}_1^{\prime(e)}$ may be expressed as

$$\mathbf{J}_1^{\prime(e)} = \frac{1}{\mu} \begin{pmatrix} \mathbf{S}_1 & & & \\ & \ddots & & \\ & & \mathbf{S}_\alpha & \\ & & & \ddots \\ & & & & \mathbf{S}_M \end{pmatrix} \cdot \mathbf{P}_1^{\prime(e)}, \tag{26}$$

where $\mathbf{S}_\alpha$ denotes the matrix $\mathbf{A}_0$ as transformed by the contraction S_α

$$\mathbf{S}_\alpha = S_\alpha(\mathbf{A}_0). \tag{27}$$

As it was discussed in section 2, we shall limit ourselves to invertible linear transformations S_α. In the simplest case of a uniform change of dimensions λ, and of Poiseuille flow in cylindrical capillaries [cf. (17)], $\mathbf{S}_\alpha$ is elementary deduced as

$$\mathbf{S}_\alpha = \lambda^{+3} \mathbf{A}_0. \tag{28}$$

In the examples detailed in the next section, λ will be usually equated to 1.

Note that an example of nonlinear transformations S_α were given in the first issue (Adler 1984 a) of this series.

The relation [26] may be briefly written with the use of a $Mn_e \times Mn_e$ matrix φ

$$\mathbf{J}_1^{\prime(e)} = \frac{1}{\mu} \varphi \cdot \mathbf{P}^{\prime(e)} \tag{29}$$

which can be rearranged as follows. Let us renumber the external flow rates and pressures as

$$\mathbf{J}_1^{\prime(e)} = \begin{pmatrix} \mathbf{J}^{\prime(e)i} \\ \mathbf{J}_1^{(e)} \end{pmatrix}, \tag{30}$$

$$\mathbf{P}_1^{\prime(e)} = \begin{pmatrix} \mathbf{P}^{\prime(e)i} \\ \mathbf{P}_1^{(e)} \end{pmatrix}. \tag{31}$$

The first $(M-1)n_e$ flow rates or pressures correspond to the $(M-1)n_e$ external vertices $v_i^{\prime(e)i}$ of Γ_1' which become internal vertices of Γ_1. The last n_e flow rates or pressures are thus relative to the n_e vertices $v_{1j}^{(e)}$ of Γ_1' which become the final external vertices of Γ_1.

Hence, the matrix φ can be subdivided into the four blocks corresponding to this distinction

$$\varphi = \begin{pmatrix} \varphi_{11} & \varphi_{12} \\ \varphi_{21} & \varphi_{22} \end{pmatrix}, \tag{32}$$

where $\varphi_{11}, \varphi_{12}, \varphi_{21}$ and φ_{22} are $(M-1)n_e \times (M-1)n_e$, $(M-1)n_e \times n_e$, $n_e \times (M-1)$ and $n_e \times n_e$ matrices, respectively. Moreover,

$$\varphi_{21} = \varphi_{12}^\dagger, \quad \varphi_{11} = \varphi_{11}^\dagger, \quad \varphi_{22} = \varphi_{22}^\dagger. \tag{33}$$

When the M subgraphs $S_\alpha\,\Gamma_0$ ($\alpha = 1, \ldots, M$) are connected according to the law symbolized by $\mathcal{T}$ [cf. [10]], it implies that the flow rates are equal and opposite (recall the algebraic convention) and that the pressures are equal at the vertices which are connected one to the other one. This may be expressed as

$$\mathcal{T} \cdot \mathbf{J}_1^{r(e)i} = -\mathbf{J}_1^{r(e)i}, \qquad [33a]$$

$$\mathcal{T} \cdot \mathbf{P}_1^{r(e)i} = \mathbf{P}_1^{r(e)i}, \qquad [33b]$$

which provide $2(M-1)n_e$ relations between the flow rates and pressures. However, exactly one half of these relations is redundant as a consequence of the symmetric character of the matrix $\mathcal{T}$. For instance, [33a] implies

$$J_{1,j_1}^{r(e)} = -J_{1,j_2}^{r(e)i}$$

and simultaneously,

$$J_{1,j_2}^{r(e)i} = -J_{1,j_1}^{r(e)i}.$$

In order to avoid these redundancies, new matrices $\mathbf{L}$ and $\mathcal{L}$ must be introduced. Let us first define the matrix $\mathcal{T}^+$ as

$$\mathcal{T}_{ij}^+ = \begin{cases} \mathcal{T}_{ij}, & i < j \\ 0, & i > j. \end{cases} \qquad [34]$$

Then $+1$ (for $\mathbf{L}$) or -1 (for $\mathcal{L}$) is added to the first diagonal of $\mathcal{T}^+$ each time that there is already 1 in the corresponding line. Then the matrices $\mathbf{L}$ and $\mathcal{L}$ are obtained by deleting the lines composed of 0 only.

This process is illustrated by the elementary example shown in figure 3.

$\mathbf{L}$ and $\mathcal{L}$ are $(M-1)(n_e/2) \times (M-1)n_e$ matrices which possess the elementary properties

$$\mathbf{L} \cdot \mathcal{L}\dagger = 0, \quad \mathbf{L} \cdot \mathbf{L}\dagger = 2\,\mathbf{I}, \quad \mathcal{L} \cdot \mathcal{L}\dagger = 2\,\mathbf{I}. \qquad [35]$$

The proof of these relations readily follows from the definition of these matrices; they may be verified in the example of figure 3.

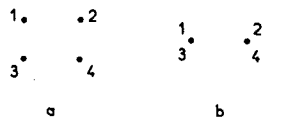

Figure 3. Illustration of the calculation of $\mathbf{L}$ and $\mathcal{L}$. Four vertices 1, 2, 3, 4 are given in (a). Then 1 is connected to 4, and 2 to 3. Hence,

$$\mathcal{T} = \begin{pmatrix} 0 & 0 & 0 & 1 \\ 0 & 0 & 1 & 0 \\ 0 & 1 & 0 & 0 \\ 1 & 0 & 0 & 0 \end{pmatrix}, \quad \mathcal{T}\dagger = \begin{pmatrix} 0 & 0 & 0 & 1 \\ 0 & 0 & 1 & 0 \\ 0 & 0 & 0 & 0 \\ 0 & 0 & 0 & 0 \end{pmatrix},$$

$$\mathbf{L} = \begin{pmatrix} 1 & 0 & 0 & 1 \\ 0 & 1 & 1 & 0 \end{pmatrix}, \quad \mathcal{L} = \begin{pmatrix} -1 & 0 & 0 & 1 \\ 0 & -1 & 1 & 0 \end{pmatrix}.$$

With the use of these two matrices, the equations [33] can be replaced by the nonredundant set of $(M-1)n_e$ relations

$$\mathbf{L} \cdot \mathbf{J}_1'^{(e)i} = 0, \tag{36a}$$

$$\mathcal{L} \cdot \mathbf{P}_1'^{(e)i} = 0, \tag{36b}$$

which completely describe the assemblages.

Of course, the vectors $\mathbf{J}_1'^{(e)i}$ ($\mathbf{P}_1'^{(e)i}$) is composed of $(M-1)n_e$ components which are two by two opposite (equal), say

$$\mathbf{J}_1'^{(e)i} = \begin{pmatrix} K_1 \\ K_2 \\ \vdots \\ -K_2 \\ \vdots \\ -K_1 \\ \vdots \end{pmatrix} \tag{37}$$

and the equivalent relation for $\mathbf{P}_1'^{(e)i}$.

This property may be phrased differently. The vectors $\mathbf{J}_1'^{(e)i}$ and $\mathbf{P}_1'^{(e)i}$ belong to the kernels of $\mathbf{L}$ and $\mathcal{L}$, respectively. It is more convenient to introduce new and nonredundant flow rate and pressure vectors $\mathbf{J}'^{i}$ and $\mathbf{P}'^{i}$, each of them possessing $(M-1)n_e/2$ independent components, and such that

$$\mathbf{J}_1'^{(e)i} = \mathcal{L}\dagger \cdot \mathbf{J}'^{i}, \tag{38a}$$

$$\mathbf{P}_1'^{(e)i} = \mathbf{L}\dagger \cdot \mathbf{P}'^{i}. \tag{38b}$$

Hence, two unknown but related values of $\mathbf{J}_1'^{(e)i}$ (or $\mathbf{P}_1'^{(e)i}$) correspond to one unknown value of $\mathbf{J}'^{i}$ (or $\mathbf{P}'^{i}$). With this formulation, [36] are automatically satisfied.

4.3. *Calculation of the first iteration*

As a pleasant consequence of these lengthy preliminaries, the actual solution of the problem is now at hand.

Introduction of [30] and [32] into the general relation [29] yields

$$\mathbf{J}_1'^{(e)i} = \frac{1}{\mu}(\varphi_{11} \cdot \mathbf{P}'^{(e)i} + \varphi_{12} \cdot \mathbf{P}_1^{(e)}), \tag{39a}$$

$$\mathbf{J}_1^{(e)} = \frac{1}{\mu}(\varphi_{21} \cdot \mathbf{P}'^{(e)i} + \varphi_{22} \cdot \mathbf{P}_1^{(e)}). \tag{39b}$$

[39a] is composed by $(M-1)n_e$ relations and [39b] by n_e relations.

The solution is obtained as follows. [39a] furnishes $(M-1)n_e/2$ relations, from which the components of the vector $\mathbf{P}'^{i}$ can be deduced. Introduction of these values into [39b] yields the desired relation between $\mathbf{J}_1^{(e)}$ and $\mathbf{P}_1^{(e)}$.

Let us now detail and discuss this solution. When [39a] is multiplied at its left by $\mathbf{L}$, its left-hand side vanishes as a consequence of [36a]. Introduction of [38b] yields

$$\mathbf{L} \cdot \varphi_{11} \cdot \mathbf{L}\dagger \cdot \mathbf{P}'' + \mathbf{L} \cdot \varphi_{12} \cdot \mathbf{P}_1^{(e)} = 0. \qquad [40]$$

This matricial equality is equivalent of $(M-1)n_e/2$ relations between the $(M-1)n_e/2$ independent components of $\mathbf{P}''$. They can be calculated in function of $\mathbf{P}_1^{(e)}$ when $\mathbf{L} \cdot \varphi_{11} \cdot \mathbf{L}\dagger$ is invertible, a property which is now discussed.

The matrix $\mathbf{L} \cdot \varphi_{11} \cdot \mathbf{L}\dagger$ is square, symmetric and has $(M-1)n_e/2$ lines and rows. On intuitive grounds, it is expected to be invertible since one should not encounter any difficulty in solving the corresponding physical problem, which is equivalent to the calculation of the pressure at some inner vertices, in function of the pressures in a connected graph.

This qualitative argument may be sharpened as follows. Actually, the trouble is mostly of a technical character, which is related to the invertibility of the matrix $\mathbf{a}_0$, and to the non-invertibility of $\mathbf{A}_0$. First, suppose that the graph Γ_1 is composed of $n_e = M$ subgraphs $S_\alpha\Gamma_0$, each of them having one and only one vertex which becomes an external vertex of Γ_1. Hence, in a given subgraph $S_\alpha\Gamma_0$, the origin of pressure may be assigned to this external vertex. When φ is rearranged according to [32], the part of $\mathbf{S}_\alpha$ which remains in φ_{11} is invertible since it is $S_\alpha(\mathbf{a}_0)$. Hence, φ_{11} is invertible, since it is composed by $n_e - 1$ blocks which are themselves invertible.

Second, suppose that M is strictly larger than n_e; thus, some subgraphs $S_\alpha\Gamma_0$ do not possess any external vertex of Γ_1. However, since Γ_1 is assumed to be connected (see section 2), these internal subgraphs may each be linked to at least one subgraph with one external vertex. When this is done for all the internal subgraphs, we are back in the first case.

Third, it may happen that one subgraph $S_\alpha\Gamma_0$ has two or more external vertices. This subgraph may be subdivided into parts having each only one external vertex of Γ_1 and thus we are back in the second case.

Hence, we may write

$$\mathbf{P}'' = -(\mathbf{L} \cdot \varphi_{11} \cdot \mathbf{L}\dagger)^{-1} \cdot \mathbf{L} \cdot \varphi_{12} \cdot \mathbf{P}_1^{(e)}. \qquad [41]$$

Introduction of this equality and of [38b] into [39b] yields the final result

$$\mathbf{J}_1^{(e)} = \frac{1}{\mu}[-\varphi_{21} \cdot \mathbf{L}\dagger \cdot (\mathbf{L} \cdot \varphi_{11} \cdot \mathbf{L}\dagger)^{-1} \cdot \mathbf{L} \cdot \varphi_{12} + \varphi_{22}] \cdot \mathbf{P}_1^{(e)} \qquad [42]$$

which is the desired relation between $\mathbf{J}_1^{(e)}$ and $\mathbf{P}_1^{(e)}$ according to the definition [20a] of $\mathbf{A}_1$, we obtain

$$\mathbf{A}_1 = -\varphi_{12}^{\dagger} \cdot \mathbf{L}\dagger \cdot (\mathbf{L} \cdot \varphi_{11} \cdot \mathbf{L}\dagger)^{-1} \cdot \mathbf{L} \cdot \varphi_{12} + \varphi_{22} \qquad [43]$$

which is satisfactory both by its generality and compacity. It is obviously symmetric in view of [33]. From the previous developments, it must be reminded that $\mathbf{A}_1$ is not invertible.

4.4. *The general iteration formula*

Now we are in a convenient position to detail the functional relation between $\mathbf{A}_0$ and $\mathbf{A}_1$ as it was expressed by $\mathbf{F}$ in [21a]. In order to do that, the relation between φ and $\mathbf{A}_0$ must be explicited since it was somewhat masked by the general expression φ.

As previously stated, the transformation S_α has been assumed to be a linear operator [cf. [27]]; hence,

$$\mathbf{S}_\alpha = \mathbf{s}_\alpha \cdot \mathbf{A}_0, \qquad [46]$$

where $\mathbf{s}_\alpha$ is a $n_e \times n_e$ matrix.

Then, φ may be expressed as

$$\varphi = \mathbf{S} \cdot \mathbf{E} : \mathbf{A}_0, \tag{45}$$

where $\mathbf{S}$ is a $Mn_e \times Mn_e$ second-order tensor, which can be written as

$$\mathbf{S} = \begin{pmatrix} \mathbf{s}_1 & & & \\ & \ddots & & \\ & & \mathbf{s}_\alpha & \\ & & & \ddots \\ & & & & \mathbf{s}_M \end{pmatrix}. \tag{46}$$

$\mathbf{E}$ is a $Mn_e \times Mn_e \times n_e \times n_e$ fourth-order tensor such as the matrix $\mathbf{A}_0$ is replicated M times

$$\mathbf{E} : \mathbf{A}_0 = \begin{pmatrix} \mathbf{A}_0 & & \\ & \ddots & \\ & & \mathbf{A}_0 \end{pmatrix}. \tag{47}$$

Introduction of [46] and [47] into [45] obviously yields an identity. The general component of the fourth-order tensor may be expressed as

$$E_{ijkl} = \delta\left[\frac{i}{n_e}\right], \left[\frac{j}{n_e}\right] \cdot \delta_{(i),k} \cdot \delta_{(j),l}, \tag{48}$$

where $[x]$ denotes the integral part of x and (i) the value of i modulo n_e. The Kronecker symbol is equal to 1 when its two arguments are equal, zero otherwise. This complicated expression automatically ensures the replication of $\mathbf{A}_0$ according to [47].

Then, φ was rearranged into blocks in order to leave at its ends the vertices which become the external vertices of Γ_1 [cf. [32]]. According to [45] a permutation of the indices of φ corresponds to a permutation of the first index of $\mathbf{S}$ and of the second index of $\mathbf{E}$. When these two indices are ranging from 1 to $(M-1)n_e$, and from $(M-1)n_e + 1$ to Mn_e, the tensors $\mathbf{S}_1$, $\mathbf{E}_1$ and $\mathbf{S}_2$, $\mathbf{E}_2$ are obtained respectively. Hence,

$$\varphi_{ij} = \mathbf{S}_i \cdot \mathbf{E}_j : \mathbf{A}_0 \quad (i, j = 1, 2). \tag{49}$$

Introduction of [49] into [43] yields the general expression

$$\mathbf{A}_1 = -(\mathbf{S}_2 \cdot \mathbf{E}_1 : \mathbf{A}_0) \cdot \mathbf{L}\dagger \cdot [\mathbf{L} \cdot (\mathbf{S}_1 \cdot \mathbf{E}_1 : \mathbf{A}_0) \cdot \mathbf{L}\dagger]^{-1} \cdot \mathbf{L} \cdot \mathbf{S}_1 \cdot \mathbf{E}_2 : \mathbf{A}_0 + \mathbf{S}_2 \cdot \mathbf{E}_2 : \mathbf{A}_0. \tag{50}$$

The details which are given in this formula certainly obscure the general form of the relationship between $\mathbf{A}_1$ and $\mathbf{A}_0$ so its derivation was not presented first. However, it has the definite advantage of being immediately extrapolated to the relation between $\mathbf{A}_N$ and $\mathbf{A}_{N-1}$. This relation is merely a duplication of [50] and reads as

$$\mathbf{A}_N = -(\mathbf{S}_2 \cdot \mathbf{E}_1 : \mathbf{A}_{N-1}) \cdot \mathbf{L}\dagger \cdot [\mathbf{L} \cdot (\mathbf{S}_1 \cdot \mathbf{E}_1 : \mathbf{A}_{N-1}) \cdot \mathbf{L}\dagger]^{-1} \cdot \mathbf{L} \cdot \mathbf{S}_1 \cdot \mathbf{E}_2 : \mathbf{A}_{N-1} + \mathbf{S}_2 \cdot \mathbf{E}_2 : \mathbf{A}_{N-1}. \tag{51}$$

Hence, as it was stated at the beginning of this section, one of the primary purposes of this paper is fulfilled with the explicit relation [51] between $\mathbf{A}_{N-1}$ and $\mathbf{A}_N$, i.e. between two successive steps in the construction of the fractal.

4.5. *The fractal relation*

The function **F** [cf. [21a]] corresponding to the general iteration formula [51] is obviously nonlinear and thus many different phenomena may happen depending upon the particular character of the transformations involved.

An important simplification occurs when this function **F** is a linear function or can be linearized, in such a way that the iteration formula [51] may be written as

$$\mathbf{A}_N = \mathcal{F} : \mathbf{A}_{N-1}, \qquad [52]$$

where $\mathcal{F}$ is a fourth-order tensor that we shall call the fractal tensor.

Let us now briefly investigate when such a relation can be obtained and how it may be deduced from [51]. First, we shall assume that the function **F** has a fixed point $\mathbf{A}_\infty$, i.e.

$$\mathbf{A}_\infty = \mathbf{F}(\mathbf{A}_\infty). \qquad [53]$$

In many cases, such a fixed point is located at the origin, i.e. $\mathbf{A}_\infty = 0$. Consider, for instance, a wire mesh which is steadily increased by successive additions of wires (as the Sierpinski gasket that is considered in the next section); when the pressures are held constant at the external vertices, the flow rates tend towards zero, from which fact the existence of a fixed point is suspected at zero.

Fixed points may also appear for finite values of $\mathbf{A}_\infty$. For instance, a fractal may be defined in such a way that the distance between two external vertices is not modified; a finite fixed point is then expected on intuitive grounds. However, the former situation can be obtained with an origin shift.

Serious problems may arise when the unicity of fixed points is examined, not to speak about their existence. We shall not deal with these questions here, especially in view of the potential applications where the transformations S_α ($\alpha = 1, \ldots, M$) are not linear. In the following, we assume that the starting "point," represented by the tensor $\mathbf{A}_0$, is located in the neighbourhood of a given fixed point $\mathbf{A}_\infty = 0$ which is progressively reached by successive applications of **F**.

Let us further assume that **F** is differentiable at the origin; it is then an easy matter to realize that the fractal tensor $\mathcal{F}$ is the gradient of **F** at the origin

$$\mathcal{F} = \left.\frac{\partial \mathbf{F}}{\partial \mathbf{A}}\right|_{\mathbf{A}=0}. \qquad [54]$$

Then [52] corresponds simply to the first-order term of the Taylor expansion of **F** near the origin. For sake of clarity, the situation is illustrated in figure 4 for the one dimensional case.

The fractal tensor $\mathcal{F}$ may be obtained in several ways. The easiest one consists in the elementary differentiation of the function **F**, i.e.

$$\mathcal{F}_{ijkm} = \left.\frac{\partial F_{ij}}{\partial A_{km}}\right|_{\mathbf{A}=0}. \qquad [55]$$

An alternate way consists in using the formal tensor differentiation formula as it is given for instance by Truesdell & Noll (1965).

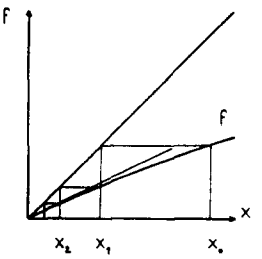

Figure 4. Illustration of the iteration process for a one-dimensional situation where F is equal to $f(x)$. The result of the successive iterations are $x_1 = f(x_0), \ldots, x_n = f^n(x_0)$; this may be geometrically obtained with the help of the first intersect (the upper straight and broad line). When x is small enough, $f(x)$ may be approximated by its tangent $f'(0) \cdot x$ (the thin line). The fractal constant is equal to $f'(0)$.

5. EXAMPLES

In order to illustrate both the construction mechanism and the application of the general formulae [51] and [52], two examples are fully explicited. The first one is the classical Sierpinski gasket. The second one is less classical, but represents a structure of importance both in polymer adsorption on a solid wall and in the injection of a fluid in a porous medium.

5.1. *The Sierpinski gasket and its extension*

The construction process is well known and is illustrated in figure 5. The initial "pressure drop flow rate conductivity" coefficients are all equal to 1 in the isotropic gasket; for sake of convenience, dimensionless pressures, flow rates . . . are used; the viscosity of the fluid is also equal to 1.

The relation between the flow rates going out of the basic graph Γ_0 [cf. figure 5a] and the pressures at the external vertices may be derived from elementary arguments as

$$\begin{pmatrix} J_1 \\ J_2 \\ J_3 \end{pmatrix} = \begin{pmatrix} -2 & 1 & 1 \\ 1 & -2 & 1 \\ 1 & 1 & -2 \end{pmatrix} \cdot \begin{pmatrix} P_1 \\ P_2 \\ P_3 \end{pmatrix}. \qquad [56]$$

The relations between the vertices of the three basic graphs Γ_0 when they are assembled to give the graph Γ_1 (cf. figure 5b) are symbolized by the matrix $\mathcal{T}$

$$\mathcal{T} = \begin{pmatrix} 0 & 0 & 1 & 0 & 0 & 0 \\ 0 & 0 & 0 & 0 & 1 & 0 \\ 1 & 0 & 0 & 0 & 0 & 0 \\ 0 & 0 & 0 & 0 & 0 & 1 \\ 0 & 1 & 0 & 0 & 0 & 0 \\ 0 & 0 & 0 & 1 & 0 & 0 \end{pmatrix}. \qquad [57]$$

The internal vertices are assumed to be ordered according to their increasing number, i.e. 2, 3, 4, 6, 7 and 8.

L is then deduced according to the process described in the previous section; hence

$$\mathbf{L} = \begin{pmatrix} 1 & 0 & 1 & 0 & 0 & 0 \\ 0 & 1 & 0 & 0 & 1 & 0 \\ 0 & 0 & 0 & 1 & 0 & 1 \end{pmatrix}. \qquad [58]$$

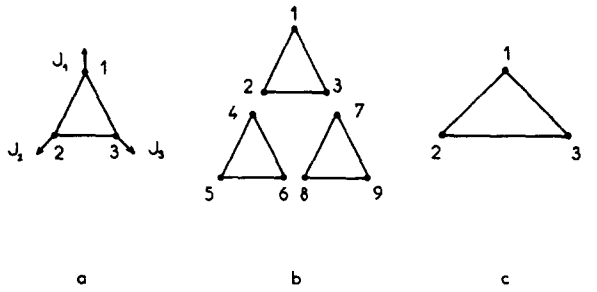

Figure 5. The construction process of the isotropic Sierpinski gasket. The basic graph Γ_0 is given in (a); three basic graphs are used to construct Γ_1' as it is shown in (b). The basic graph of the anisotropic case in given in (c) and the construction process is the same as in the previous situation.

For the sake of clarity, the three transformations s_1, s_2 and s_3 are assumed to be the identity. Hence, the matrix φ is obtained by the juxtaposition of three matrices A_0, as given by [56]. Let us order the external vertices of Γ_1 as 1, 5, 9 (cf. figure 5b); the internal vertices of Γ_1 are ordered according to the previous convention 2, 3, 4, 6, 7, 8. The matrices φ_{11}, $\varphi_{12}(=\varphi_{21}^{\dagger})$ and φ_{22} are derived from φ as

$$\varphi_{11} = \begin{pmatrix} -2 & 1 & 0 & 0 & 0 & 0 \\ 1 & -2 & 0 & 0 & 0 & 0 \\ 0 & 0 & -2 & 1 & 0 & 0 \\ 0 & 0 & 1 & -2 & 0 & 0 \\ 0 & 0 & 0 & 0 & -2 & 1 \\ 0 & 0 & 0 & 0 & 1 & -2 \end{pmatrix},$$

$$\varphi_{12} = \begin{pmatrix} 1 & 0 & 0 \\ 1 & 0 & 0 \\ 0 & 1 & 0 \\ 0 & 1 & 0 \\ 0 & 0 & 1 \\ 0 & 0 & 1 \end{pmatrix}, \varphi_{22} = \begin{pmatrix} -2 & 0 & 0 \\ 0 & -2 & 0 \\ 0 & 0 & -2 \end{pmatrix}. \quad [59]$$

It is now a simple matter for the reader to perform the calculations as they are given by [43]; we obtain

$$\mathbf{L} \cdot \varphi_{11} \cdot \mathbf{L}\dagger = \begin{pmatrix} -4 & 1 & 1 \\ 1 & -4 & 1 \\ 1 & 1 & -4 \end{pmatrix}$$

whose inversion is immediate

$$(\mathbf{L} \cdot \varphi_{11} \cdot \mathbf{L}\dagger)^{-1} = -\frac{1}{10}\begin{pmatrix} 3 & 1 & 1 \\ 1 & 3 & 1 \\ 1 & 1 & 3 \end{pmatrix}.$$

$\mathbf{A}_1$ is obtained after a few more steps as

$$\mathbf{A}_1 = \frac{3}{5}\begin{pmatrix} -2 & 1 & 1 \\ 1 & -2 & 1 \\ 1 & 1 & -2 \end{pmatrix},$$

i.e. the result

$$\mathbf{A}_1 = 3/5\,\mathbf{A}_0 \tag{60a}$$

which can be readily derived by an application of the classical startriangle transformation. It is very gratifying to derive this expected 3/5 coefficient through the general formalism worked out in section 4.

The function $\mathbf{F}$ is thus very simple, since it is reduced to the multiplication by the spherical tensor $3/5 \cdot \mathbf{I}$. The fractal tensor $\mathcal{F}$ is "equal" to the constant 3/5. It will be seen below that the linear character of the relation [60] is related to the isotropy of the Sierpinsky gasket as shown in figures 5a and 5b.

If the transformations S_α were not the identity anymore, but given by [28] for instance, then the relation [60a] would have to be modified as

$$\mathbf{A}_1 = 3/5 \cdot \lambda^{+3}\,\mathbf{A}_0. \tag{60b}$$

Let us now investigate the influence of anisotropy on the iteration formula. The simplest extension of the previous gasket is shown in figure 5c. Two sides of the basic graph Γ_0 have equal resistances (arbitrary equated to 2); the third side has a resistance α'. First, it is possible to show by symmetry arguments that $\mathbf{A}_N$ has the general form

$$\mathbf{A}_N = \begin{pmatrix} -2\,\alpha_N & \alpha_N & \alpha_N \\ \alpha_N & a_N & b_N \\ \alpha_N & b_N & a_N \end{pmatrix}, \tag{61}$$

where $\alpha_N = -(a_N + b_N)$. The initial values of a_0 and b_0 are equal to

$$\begin{aligned} a_0 &= -0.5 - 1./\alpha', \\ b_0 &= 1./\alpha' \end{aligned} \tag{62}$$

as it may be shown by analysis of the basic graph Γ_0.

The iteration process may be summed up by the formulae

$$\begin{aligned} \Delta_N &= 2[a_N(a_N - 2\,\alpha_N)^2 + b_N\,\alpha_N^2 - \alpha_N^2(a_N - 2\,\alpha_N) - b_N^2\,a_N], \\ Y_N &= 2\,b_N\,\alpha_N^2(b_N - a_N + 2\,\alpha_N) + b_N^2(a_N - 2\,\alpha_N)^2 - b_N^4, \\ a_{N+1} &= -\frac{1}{\Delta_N} \cdot \{\alpha_N^2 \cdot [2\,a_N(a_N - 2\,\alpha_N) - \alpha_N^2] + Y_N\} + a_N, \\ b_{N+1} &= -\frac{1}{\Delta_N} \cdot \{\alpha_N^2(\alpha_N^2 - 2\,a_N\,b_N) + Y_N\}. \end{aligned} \tag{63}$$

This iteration is illustrated in figure 6 for various values of the anisotropy parameter $\alpha'/2$.

Several comments may be offered on these results. Note first that the Sierpinski gasket can also be calculated as an application of the classical star-triangle transformation, which

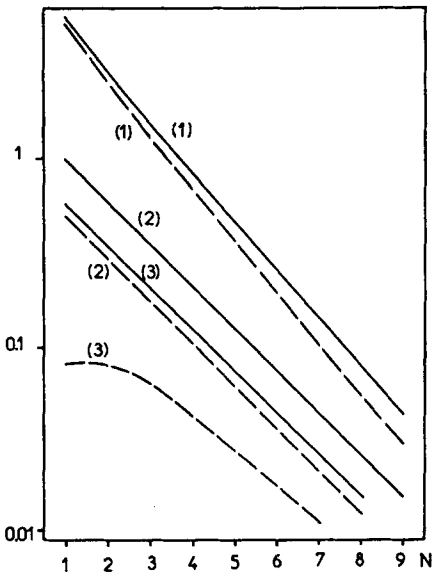

Figure 6. The coefficient $-a$ (solid lines) and b (broken lines) as functions of the number of iterations N. Values of α': 0.2 (1), 2 (2), 12 (3).

was extensively used by Adler (1984) in the Leibniz packing. This alternative route to [63] was actually used in order to check both our analytical and numerical results.

Usually, the fractal character is only obtained after several iterations. This is a direct consequence of the "nonlinearity" of [63], which is actually induced by the anisotropy of the gasket. However, the fractal limit is generally obtained pretty rapidly, i.e. after a few iterations; this feature was already present in our previous paper (Adler 1984).

Finally, the fractal coefficient is always equal to 3/5, irrespective of the degree of anisotropy as measured by the value of the coefficient α'. Hence, it depends upon the structure of the iteration process and not upon the particular values of the coefficient which is under consideration.

This may be proved in the following way, as suggested by one of the referees. The iteration formulae [63] possess a solution of the form

$$a_N = K_1 p^N, \quad b_N = K_2 p^N.$$

By substitution into [63], the values of K_2/K_1 and p can be obtained. It is easily shown that they do not depend upon α'. K_2/K_1 is the solution of the equation

$$\left(2 \cdot \frac{K_2}{K_1} + 1\right) \cdot \left[\left(\frac{K_2}{K_1}\right)^2 - 1\right] = 0,$$

that is to say

$$\frac{K_2}{K_1} = +1, -1, -\frac{1}{2},$$

$$p = \frac{4\left(\frac{K_2}{K_1}\right)^2 + 3 \cdot \frac{K_2}{K_1} - 7}{2\left(\frac{K_2}{K_1} + 3\right)\left(\frac{K_2}{K_1} - 2\right)} = 0, \frac{1}{2}, \frac{3}{5}.$$

Only the last value 3/5 is obtained from the numerical data. Note that, in figure 6, the final ratio $-1/2$ is not always obtained after nine iterations.

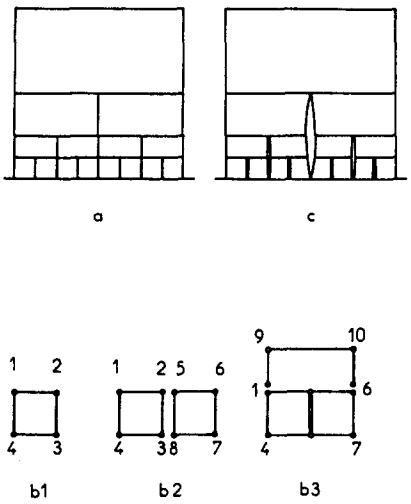

Figure 7. Injection of a fluid into a porous medium. The fractal considered in the references is shown in (a). For sake of convenience, it is replaced by the fractal (c) with the construction process described by b1, b2, b3.

5.2. *Injection of a fluid into a porous medium*

For fractal structures, a second typical situation is found in physical problems where the correlation length of the structure is equal, or related to the distance to a line or a wall (in two- and three-dimensional problems, respectively). The picture may be drastically schematized by the structure represented in figure 7a. The "radius" of the loops is equal to the distance of the center of the loop to the wall. This has already been used and discussed by De Gennes in two very different physical contexts. The first one corresponds to the adsorption of a polymer coil onto a wall (De Gennes 1979); it will not be discussed here and its analysis is postponed to a future issue of this series when flow in continuous fractal structures is studied. The second one is of very high interest here, since it happens when a fluid is injected into a porous medium (De Gennes 1983). A first approximation consists in the representation of the porous medium by a square lattice of capillaries; the injection of a fluid thus yields the picture given in figure 7a.

However, such a structure cannot be exactly obtained by the process which has been described in the previous sections. It differs from it in two aspects. An external part, that will be called the hat for obvious reasons has to be added to complete a generation; this can be easily incorporated in the theory, and the example is worked out below with this original feature. Moreover, some edges should be deleted and the equality (within a sign change) of flow rates and pressures should be written at an increasing number of vertices.

This second feature has not been incorporated in the example (we shall come back to this point at the end of this section). The fractal shown in figure 7c is obtained in lieu of the one shown in figure 7a; the construction process is illustrated in figures 7b1, 7b2 and 7b3.

Using elementary arguments, the linear relation between the outgoing flow rates and the pressures at the four external vertices (cf. figure 7b1) may be expressed as

$$\begin{pmatrix} J_1 \\ J_2 \\ J_3 \\ J_4 \end{pmatrix} = \begin{pmatrix} -2 & 1 & 0 & 1 \\ 1 & -2 & 1 & 0 \\ 0 & 1 & -2 & 1 \\ 1 & 0 & 1 & -2 \end{pmatrix} \cdot \begin{pmatrix} p_1 \\ p_2 \\ p_3 \\ p_4 \end{pmatrix}. \qquad [64]$$

As in the previous examples, all the quantities are assumed to be dimensionless and all the resistances in the initial square are equal to 1.

Let us now describe the iteration procedure. The union of two squares (cf. figure 7b2) is described by the matrices $\mathcal{T}$ and $\mathbf{L}$

$$\mathcal{T} = \begin{pmatrix} 0 & 0 & 1 & 0 \\ 0 & 0 & 0 & 1 \\ 1 & 0 & 0 & 0 \\ 0 & 1 & 0 & 0 \end{pmatrix}, \quad \mathbf{L} = \begin{pmatrix} 1 & 0 & 1 & 0 \\ 0 & 1 & 0 & 1 \end{pmatrix}, \tag{65}$$

where the internal vertices in Γ_1 have been arranged in the order 2, 3, 5, 8.

When the vertices in Γ'_1 which become external vertices in Γ'_1 are arranged in the order 1, 4, 6, 7, the matrix φ can be decomposed into four equal blocks

$$\varphi_{11} = \begin{pmatrix} A_N(1,1) & A_N(1,4) & 0 & 0 \\ A_N(4,1) & A_N(4,4) & 0 & 0 \\ 0 & 0 & A_N(2,2) & A_N(2,3) \\ 0 & 0 & A_N(3,2) & A_N(3,3) \end{pmatrix}, \tag{66a}$$

$$\varphi_{12} = \varphi_{21}^{\dagger} = \begin{pmatrix} A_N(1,2) & A_N(1,3) & 0 & 0 \\ A_N(4,2) & A_N(4,3) & 0 & 0 \\ 0 & 0 & A_N(2,1) & A_N(2,4) \\ 0 & 0 & A_N(3,1) & A_N(3,4) \end{pmatrix}, \tag{66b}$$

$$\varphi_{22} = \begin{pmatrix} A_N(2,2) & A_N(2,3) & 0 & 0 \\ A_N(3,2) & A_N(3,3) & 0 & 0 \\ 0 & 0 & A_N(1,1) & A_N(1,4) \\ 0 & 0 & A_N(4,1) & A_N(4,4) \end{pmatrix}. \tag{66c}$$

Hence, when the calculations described by [43] are performed, we can obtain the relation (corresponding to the situation illustrated in figure 7b2)

$$\begin{pmatrix} J_1 \\ J_6 \\ J_7 \\ J_4 \end{pmatrix} = \begin{pmatrix} \mathbf{A}'_N & \mathbf{B}'_N \\ \mathbf{C}'_N & \mathbf{D}'_N \end{pmatrix} \cdot \begin{pmatrix} p_1 \\ p_6 \\ p_7 \\ p_4 \end{pmatrix}. \tag{67}$$

where $\mathbf{A}'_N$, $\mathbf{B}'_N$, $\mathbf{C}'_N$ and $\mathbf{D}'_N$ are 2×2 matrices.

The "hat" [1, 9, 10, 6] has to be added in order to finish the construction of the fractal. Consistently, the resistances of the edges [1, 9], [9, 10] and [10, 6] are equal to 2^{N-1}, 2^N and 2^{N-1}, respectively at the step N. The intermediate variables (J_1, J_6) and (P_1, P_6) can be expressed as functions of J_9, J_{10} and P_9, P_{10} by expressing the flow rate conservation at each vertex and the Ohm's law along each edge. Hence,

$$\begin{pmatrix} J_1 \\ J_6 \end{pmatrix} = \begin{pmatrix} J_9 \\ J_{10} \end{pmatrix} + \frac{1}{2^N} \cdot \begin{pmatrix} 1 & -1 \\ -1 & 1 \end{pmatrix} \begin{pmatrix} P_9 \\ P_{10} \end{pmatrix}, \tag{68.a}$$

$$\begin{pmatrix} P_1 \\ P_6 \end{pmatrix} = 2^{N-1} \cdot \begin{pmatrix} J_9 \\ J_{10} \end{pmatrix} + \begin{pmatrix} \frac{3}{2} & -\frac{1}{2} \\ -\frac{1}{2} & \frac{3}{2} \end{pmatrix} \begin{pmatrix} P_9 \\ P_{10} \end{pmatrix} \qquad [68.b]$$

when the four intermediate variables are eliminated between [67] and [68], the final relation between the flow rates and pressures may be expressed as

$$\begin{pmatrix} J_9 \\ J_{10} \\ J_7 \\ J_4 \end{pmatrix} = \begin{pmatrix} \alpha_N & \beta_N \\ \gamma_N & \delta_N \end{pmatrix} \begin{pmatrix} P_9 \\ P_{10} \\ P_7 \\ P_4 \end{pmatrix}, \qquad [69]$$

where the 2×2 matrices α_N, β_N, γ_N and δ_N are given by

$$\begin{aligned} \alpha_N &= (\mathbf{I} - 2^{N-1} \cdot \mathbf{A}'_N)^{-1} \cdot \left[\mathbf{A}'_N \cdot \begin{pmatrix} \frac{3}{2} & -\frac{1}{2} \\ -\frac{1}{2} & \frac{3}{2} \end{pmatrix} - \frac{1}{2^N} \cdot \begin{pmatrix} 1 & -1 \\ -1 & 1 \end{pmatrix} \right], \\ \beta_N &= (\mathbf{I} - 2^{N-1} \cdot \mathbf{A}'_N)^{-1} \cdot \mathbf{B}'_N, \\ \gamma_N &= \mathbf{C}'_N \cdot \left[2^{N-1} \alpha_N + \begin{pmatrix} \frac{3}{2} & -\frac{1}{2} \\ -\frac{1}{2} & \frac{3}{2} \end{pmatrix} \right], \\ \delta_N &= 2^{N-1} \mathbf{C}'_N \cdot \beta_N + \mathbf{D}'_N. \end{aligned} \qquad [70]$$

Of course, $\mathbf{A}_N$ is equal to the matrix in [69]. We can come back to the starting point, the matrix φ as expressed by [66], and we can reiterate the construction of the fractal.

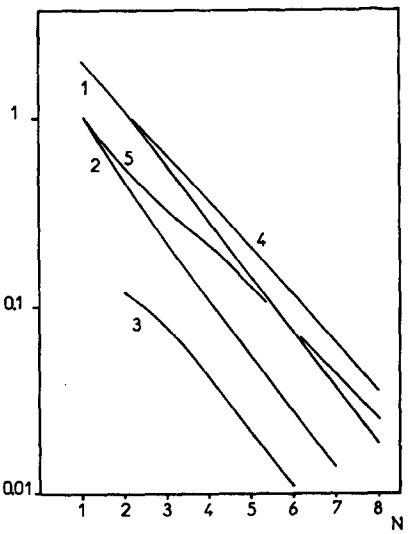

Figure 8. The five independent coefficients $-A_N$ (2, 2) (a), A_N (2, 3) (b), A_N (2, 4) (c), $-A_N$ (3, 3) (d) and A_N (3, 4) (e) as a function of the iteration number N for the injection of a fluid into a porous medium.

These calculations are best done by a computer; when the initial matrix $\mathbf{A}_0$ is [64], results are illustrated in figure 8 when the five independent coefficients of $\mathbf{A}_N$ are given as a function of the iteration number N. This reduction in the number of independent coefficients of $\mathbf{A}_N$ is a consequence of its symmetric character, of the fact that the sum of every row (or line) is zero and of the symmetry of the graph.

Comments could be very similar to the ones given for the Sierpinski gasket. Some nonlinearity is also present and its amount depends upon the coefficient under consideration. The fractal character is only reached in the limit. The fractal tensor seems to be reducible to a single coefficient which was numerically found to be close to 0.5; note that $A_N(3, 4)$ eventually reaches this trend after a large number of iterations (~20).

Finally, let us examine the network represented in figure 7a. As it was already emphasized, it is an idealization of the physical situation. However, we are really interested by the pressures and flow rates at the corners, since the fluid invades larger structures from these corners. The network of figure 7a can be obtained by deleting some edges at each step; simultaneously, the equality of pressures and flow rates should be written at an increasing number of vertices. For instance, in figure 7b2, the edge 2-3 has to be deleted. In figure 7b3, two different situations must be calculated in order to obtain the next generation; first, the graph is complete and the external vertices are 4, 7, 6, 10 and 9; second, the external vertices are 4, 1, 9, 10 and 7, while the edges (1-4) and (1-9) are deleted. This process can be repeated.

6. DISCUSSION

As it was already stated in the previous section, the construction process can be generalized in many ways. Edges and vertices may be deleted, as it would be actually necessary for a rigorous construction process of the injection shown in figure 7a. Some finite graph, which was called the hat in this example, can be added at each step. This last feature illustrated in section 5.2 is not difficult to generalize.

There is an other possible extension which is not *a priori* obvious. In the above theory, all the flow occurs, so to speak, around the fractal, since the network is always energized by the external vertices. We can also think of a different situation where the flow would occur between the external vertices of Γ_N and the external vertices of an inner graph, say $S_\alpha\Gamma_0$. More precisely, the inner graph $S_\alpha\Gamma_0$ is deleted, and external pressures $\mathbf{P}^{(e)}_{0,\alpha}$ and flow rates $\mathbf{J}^{(3)}_{0,\alpha}$ are imposed at its corresponding external vertices. The relation [22a] can be generalized as

$$\begin{pmatrix} \mathbf{J}^{(e)}_N \\ \mathbf{J}^{(e)}_{0,\alpha} \end{pmatrix} = \frac{1}{\mu} \mathbf{A}_N \cdot \begin{pmatrix} \mathbf{P}^{(e)}_N \\ \mathbf{P}^{(e)}_{0,\alpha} \end{pmatrix}, \qquad [71]$$

where the $2n_e \times 2n_e$ matrix $\mathbf{A}_N$ has to be calculated. This situation was not further investigated, since it is usually the one described by [22a] which is of practical significance.

The relation [43] presents some formal similarity with the general formula obtained by Adler & Brenner (1984a) for a spatially periodic capillary network, since in both cases there is a central inverted matrix. The same basic ingredients are present in some sense; the internal arrangement of the local graph was symbolized by a cycle matrix $\mathbf{C}$ (here φ); the relations between the various unit cells were represented by a mixed operator $\mathcal{R}$ (here $\mathbf{L}$).

This provides us with a useful transition to the next point of the discussion. For spatially periodic networks, the flow rate vector was assumed to be spatially periodic. As a direct consequence, the pressure field could be decomposed into a continuous component related to the macroscopic pressure drop and a spatially periodic component. In the present situation, it is equivalent to relate the pressure vector $\mathbf{P}^{\prime(e)i}_{N-1}$ (the flow rate vector $\mathbf{J}^{\prime(e)i}_{N-1}$) at the external vertices of Γ'_N which become internal vertices of Γ_N to the pressure vector $\mathbf{P}^{(e)}_N$ (the flow rate vector $\mathbf{J}^{(e)}_N$) at the external vertices of Γ_N.

As a consequence of the fundamental linearity of the Stokes flow on a capillary network, linear relations exist between these quantities

$$\mathbf{P}'^{(e)i}_{N-1} = \mathbf{G}_N \cdot \mathbf{P}^{(e)}_N, \tag{72a}$$

$$\mathbf{J}'^{(e)i}_{N-1} = \mathbf{H}_N \cdot \mathbf{J}^{(e)}_N, \tag{72b}$$

where $\mathbf{G}_N$ and $\mathbf{H}_N$ are $(M-1)n_e \times n_e$ matrices. Physically, these relations mean that internal quantities can be calculated when the external and controlling quantities are known.

These two matrices can be calculated as functions of the basic elements of description of the construction process. The matrix $\varphi^{(N-1)}$ may be defined as a generalization of the matrix φ [cf. [32]] when its constitutive elements are based upon $\mathbf{A}_{N-1}$. Thus, [39a] can be generalized into

$$\mathbf{J}'^{(e)i}_{N-1} = \frac{1}{\mu}(\varphi^{(N-1)}_{11} \cdot \mathbf{P}'^{(e)i}_{N-1} + \varphi^{(N-1)}_{12} \cdot \mathbf{P}^{(e)}_N). \tag{73}$$

Relations which are analogous to [38], [41] and [42] can easily be written down. The general expression for $\mathbf{G}_N$ can be given as

$$\mathbf{G}_N = -\mathbf{L}\dagger \cdot (\mathbf{L} \cdot \varphi^{(N-1)}_{11} \cdot \mathbf{L}\dagger)^{-1} \cdot \mathbf{L} \cdot \varphi^{(N-1)}_{12}. \tag{74}$$

Introduction of [72b] into [73] yields

$$\mathbf{J}'^{(e)i}_{N-1} = \frac{1}{\mu}(\varphi^{(N-1)}_{11} \cdot \mathbf{G}_N + \varphi^{(N-1)}_{12}) \cdot \mathbf{P}^{(e)}_N. \tag{75}$$

Since $\mathbf{A}_N$ is not invertible, some care should be taken for the expression of $\mathbf{P}^{(e)}_N$ as a function of $\mathbf{J}^{(e)}_N$. The n^{th}_e external vertex of Γ_N can be maintained at pressure 0; hence,

$$\mathbf{p}^{(e)}_N = \mu \mathbf{a}^{-1}_N \cdot \mathbf{j}^{(e)}_N. \tag{76}$$

The corresponding flow rate does not appear as such in [72b].

Apart this minor point, the matrix $\mathbf{H}_N$ is easily derived as

$$\mathbf{H}_N = (\varphi^{(N-1)}_{11} \cdot \mathbf{G}_N + \varphi^{(N-1)}_{12}) \cdot \mathcal{A}_N, \tag{77}$$

Where $\mathcal{A}_N$ is the $n_e \times n_e$ matrix

$$\mathcal{A}_N = \begin{pmatrix} & & 0 \\ \mathbf{a}^{-1}_N & & \vdots \\ & & \vdots \\ 0 & \cdots & 0 \end{pmatrix}. \tag{78}$$

Hence, fractal relations are obtained when $\mathbf{G}_N$ and $\mathbf{H}_N$ tend towards constant matrices, when $N \to \infty$

$$\mathbf{G} = \lim_{N\to\infty} \mathbf{G}_N, \tag{79a}$$

$$\mathbf{H} = \lim_{N\to\infty} \mathbf{H}_N. \tag{79b}$$

In this limit, the pressure vector and the flow rate vector are fractal.

The isotropic Sierpinski gasket is an example which can be carried out analytically. $\varphi^{(N-1)}$ is given by

$$\varphi^{(N-1)} = (3/5)^{N-1} \cdot \varphi. \qquad [80]$$

It is easily foreseen that this multiplicative coefficient will disappear during the course of the calculation, which is the basic reason for which $\mathbf{G}_N$ and $\mathbf{H}_N$ generally tend towards constant limits. We deduce that

$$\mathbf{G}_N = \frac{1}{5} \cdot \begin{pmatrix} 2 & 2 & 1 \\ 2 & 1 & 2 \\ 2 & 2 & 1 \\ 1 & 2 & 2 \\ 2 & 1 & 2 \\ 1 & 2 & 2 \end{pmatrix}, \quad \mathbf{H}_N = \frac{1}{3} \cdot \begin{pmatrix} -1 & 1 & 0 \\ -2 & -1 & 0 \\ 1 & -1 & 0 \\ -1 & -2 & 0 \\ 2 & 1 & 0 \\ 1 & 2 & 0 \end{pmatrix}. \qquad [81]$$

Hence, it seems that we may state an important general property. Namely, in the limit $N \to \infty$, both the flow rates and pressures at the external vertices are fractal. A word of caution is necessary here since it may happen that this property does not always hold; so far we did not prove any general condition. Anyhow, this result has to be contrasted with the spatially periodic situation, where the character of these two quantities is different; the flow field is spatially periodic and the pressure is the superposition of a continuous component and of a spatially periodic component.

Dimensional effects, anisotropy and nonlinearity will not be fully discussed here and we shall restrict ourselves to a few remarks. No explicit reference has been made to the space dimension, which is an important advantage of the present constructon process. The most interesting nonlinear character is certainly the one which arises from an actual spatial construction, as it occurred for the Leibniz packing (Adler 1984); a nonlinearity induced on a network is surely somewhat artificial, when it is not related to a specific situation.

The Sierpinski gasket presents an original feature in relation with its isotropy; its fractal character is immediately obtained [cf. [60a]]. Highly symmetric graphs may have the same property; regular graphs such as the circuit graph or the complete graph (Biggs 1974) may be good candidates for Γ_0.

Finally, the end of this discussion is devoted to the calculation of the permeability of spatially periodic networks whose unit cell is a fractal. Of course, the permeability of the network could be obtained as in Adler & Brenner (1984a), but the gain of the present analysis would be lost since the whole graph Γ_N should be decomposed into cycles and so on .... Actually, the most convenient starting point is the transfer matrix q_N which is supposed to be known after the fractal analysis. Only a broad outline of the method is given.

The following notations are necessary. The cell number is referred to by a triplet $\mathbf{I}$ of integers, when a three-dimensional situation is considered; inside a cell, the vertex number is denoted by i. *A priori*, pressures and flow rates depend upon both $\mathbf{I}$ and i. However, the pressures may be decomposed as

$$p(\mathbf{I}, i) = p(i) + \mathbf{R}_\mathbf{I} \cdot \bar{\nabla}\bar{p}, \qquad [82]$$

where $p(i)$ is a spatially periodic function, $\mathbf{R}_\mathbf{I}$ the spatial position of cell $\mathbf{I}$ and $\bar{\nabla}\bar{p}$ the macroscopic gradient.

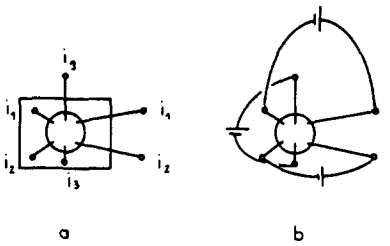

Figure 9. A spatially periodic network whose basic graph is a fractal. (a) The basic graph. (b) The derived graph with the additional edges.

Hence, the pressure drop between homologous vertices is easily found to be

$$(\mathbf{R}_{\mathrm{I}'} - \mathbf{R}_{\mathrm{I}}) \cdot \bar{\bar{\nabla}}\bar{p}. \qquad [83]$$

The derived graph $\Gamma_{N,d}$ may now be introduced by adding additional edges between the homologous vertices of Γ_N (see figure 9). To each additional edge j, a macroscopic jump vector $\mathbf{R}(j)$ may be associated

$$\mathbf{R}(j) = \mathbf{R}_{\mathrm{I}'} - \mathbf{R}_{\mathrm{I}}, \qquad [84]$$

where the edge j goes from a vertex in cell I to one in cell I'.

On this set of additional edges, a pressure generator vector may be defined as

$$\mathbf{g} = \mathcal{R} \cdot \bar{\bar{\nabla}}\bar{p}, \qquad [85]$$

where $\mathcal{R}$ is a mixed $m \times 3$ operator. Its jth line consists of the vector $\mathbf{R}(j)$†.

The graph Γ_a composed by the additional edges and the external vertices may be rearranged into its connected components; let c by their number. When the last vertex is assumed to be at pressure 0, we can decompose $\mathbf{a}_N$ into submatrices $\mathbf{a}_N^{(i,j)}$ on each component; hence, a pressure origin $\bar{p}^{(i)}$ $(i = 1, \ldots, c-1)$ can be assigned to a given vertex inside each component, except the last one. On each component, except the last one where it is automatically satisfied, the sum of the external flow rates is equal to zero. This provides $c - 1$ equations, from which $\bar{p}^{(i)}$ $(i = 1, \ldots, c-1)$ are determined.

The problem is thus solved in principle and various quantities such as the permeability can be calculated. Details are not given here since they can be found in Adler & Brenner (1984a).

REFERENCES

ADLER, P. M. 1985 Transport processes in fractals–I. Conductivity and permeability of a Leibniz packing in the lubrication limit. *Int. J. Multi. Flow*, **11**(1), 91–108.

ADLER, P. M. & BRENNER, H. 1984a Transport processes in spatially periodic capillary networks–I. Geometrical description and linear flow hydrodynamics. *PhysicoChem. Hydro.*, **5**, 245–268.

ADLER, P. M. & BRENNER, H. 1984b Transport processes in spatially periodic capillary networks–II. Taylor dispersion with mixing vertices. *PhysicoChem. Hydro.*, **5**, 269–285.

ADLER, P. M. & BRENNER, H. 1984c Transport processes in spatially periodic capillary networks–III. Nonlinear flow problems. *PhysicoChem. Hydro.*, **5**, 287–297.

ALEXANDER S. 1983 Superconductivity of networks. A percolation approach to the effects of disorder. *Phys. Rev. B***27**, 1541–57.

BIGGS, N. 1974 *Algebraic graph theory*, Cambridge University Press, Cambridge, Mass.

BOLLOBAS, B. 1979 *Graph theory: an introductory course*, Springer Verlag, New York.

DE GENNES, P. G. 1979 *Scaling concepts in polymer physics*, Cornell University Press, Ithaca, New York.

DE GENNES, P. G. 1983 Theory of slow biphasic flows in porous media. *Phys. Chem. Hydrodynamics* **4**, 175–85.

DE GENNES, P. G. & GUYON, E. 1978 Lois générales pour l'injection d'un fluide dans un milieu poreux aléatoire. *J. Mécanique* **17**, 403–32.

HAPPEL, J. & BRENNER, H. 1965 *Low Reynolds number hydrodynamics*, Prentice Hall, New Jersey.

HUTCHINSON, J. E. 1981 Fractals and self-similarity. *Indiana Univ. Math. J.* **30**, 713–47.

LARSEN, R. G., SCRIVEN, L. E. & DAVIS, H. T. 1981 Percolation theory of two phase flows in porous media. *Chem. Eng. Sci.* **36**, 57–73.

MANDELBROT, B. B. 1982 *The fractal geometry of nature*, Freeman, San Francisco.

RAMMAL, R., LUBENSKI, T. C. & TOULOUSE, G. 1983a Superconducting diamagnetism near the percolation threshold. *J. Phys. Lett.* **44**, L65–71.

RAMMAL, R., LUBENSKY, T. C. & TOULOUSE, G. 1983b Superconducting networks in a magnetic field. *Phys. Rev. B* **27**, 2820–2829.

STAUFFER, D. 1979 Scaling theory of percolation clusters, *Phys. Rep.* **54**, 1–74.

TRUESDELL, C. & NOLL, W. 1965 in *The nonlinear field theories of mechanics in Encyclopedia of Physics*, vol. III/3, edited by S. Flügge, Springer Verlag, Berlin/Heidelberg/New York.